

# A Ring Screw Mechanical Transmission Mechanism

Roy Featherstone \*

February 14, 2023

## Abstract

This document describes a new mechanical transmission mechanism, called a ring screw, that performs the same function as a ball screw but can operate at much higher speeds. It consists of a screw rod and a nut containing one or more rings that are mounted in ball bearings and make rolling contact with the screw rod when it is inserted into the nut. The special feature of the ring screw mechanism is that the shape of the screw thread in the rod, together with the shape and locations of the rings in the nut, are such that each ring makes a theoretically perfect rolling line contact with the rod. As a result, the new mechanism offers high efficiency, substantial thrust forces, high power throughput, and it can be connected directly to a modern high-speed DC motor without the need for an intervening gear reduction.

## 1 Introduction

This document describes a new mechanical device, called a ring screw, that converts fast rotary motion into slower linear motion with high power efficiency. It consists of a screw rod and a nut, the latter consisting of a frame containing one or more rings mounted in ball bearings. These rings make contact with the rod, and rotate as the rod turns relative to the nut. The shape of the thread groove in the rod, together with the shape of the rings and their placement within the nut, are such that each ring makes line contact with the rod, and its motion relative to the rod is a pure rolling motion about this line of contact. The result is a mechanism that can produce substantial thrust forces, and can transmit mechanical power with very little loss. An example of a ring screw mechanism is shown in Figure 1.

The ring screw was designed to be an alternative to a ball screw, which is a well-known mechanical component that offers a nearly frictionless screwing motion between a screw rod and a nut. It can convert a fast rotary motion, such as from an electric motor, into a slower linear motion with a power efficiency in the vicinity of 90%. However, the speed limit on a ball screw is typically around 4000–4500rpm [22, p. 36], which is far below the optimum operating speed of a modern high-speed electric motor such as a DCX or EC range motor from Maxon [16]. So an actuator employing a fast electric motor and a ball screw would typically include a gear reduction stage between the motor and the ball screw. Actuators of this kind are described in [1, 5, 11, 17, 18, 19].

The ring screw's main advantage over a ball screw is that it can operate at much higher speeds, allowing the screw rod to be connected directly to the motor's rotor shaft, thereby

---

\*Roy Featherstone was with the Department of Advanced Robotics, Italian Institute of Technology (Istituto Italiano di Tecnologia), Genoa, Italy, at the time when this work was carried out. This document is ©2023 R. Featherstone, and is available via [royfeatherstone.org/ringscrew](http://royfeatherstone.org/ringscrew).

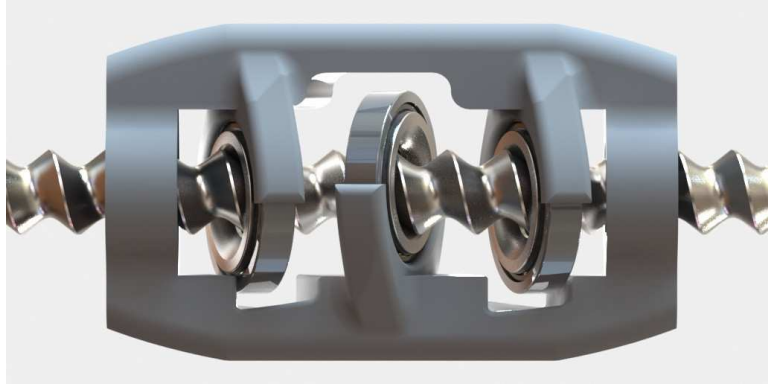


Figure 1: CAD render of a ring screw mechanism with a three-ring nut

eliminating the need for a gear reduction stage. The result is an efficient actuator with fewer moving parts. A prototype ring screw has been tested at speeds of up to 16,500rpm [13], but the device is theoretically capable of going even faster.

Another device that resembles a ball screw is the roller screw [23], which can operate at higher speeds than a ball screw and can deliver very large thrust forces. The disadvantage of the roller screw is that some of its parts have intricate shapes, making it expensive to manufacture. The ring screw cannot match the thrust force of a roller screw, but it can match or exceed the speed and efficiency, and its parts are less intricate, suggesting that it could be manufactured more cheaply.

Numerous examples exist in the patent literature of mechanisms that involve a screw rod and rotating rings, and therefore resemble a ring screw. Some of the most relevant ones are [3, 12, 14, 20]. However, none of these devices exhibit the special feature of the ring screw, which is the theoretically exact pure rolling line contact between the rod and the rings [6, 7, 8]. Operational data on these inventions does not appear to be available, but their lack of this special feature suggests that they would not be able to match the ring screw's thrust force or efficiency. The tests reported in [13] on a prototype ring screw put its efficiency at around 90%; but limitations in the test equipment meant that the prototype could not be tested at thrust forces above 800N.

The rest of this document is organized as follows. Section 2 derives the kinematic equations of the ring screw, which establish the relationships between the pitch of the screw rod, the location of an individual ring and the location of its line of rolling contact with the rod. Section 3 describes the shapes of the contacting surfaces on the rings and the screw thread groove that produce the line contact. Then Section 4 describes other aspects of the shapes of the rod and rings in the form of a practical procedure for designing a ring screw mechanism. Section 5 considers the construction and mounting of rings in their bearings, and the number and placement of rings in the nut. Finally, Section 6 considers the contact forces between the rod and the rings, and their relationship to the thrust force produced by the mechanism.

## 2 Kinematic Design

A basic result in screw theory (the theory of infinitesimal movements of rigid bodies) is that the sum of two screwing motions (twists) is another screwing motion, and that all three screw axes lie on a ruled surface called a *cylindroid* and therefore share a single common perpendicular [2, 15, 4]. As rotation is simply a screwing motion of zero pitch, it follows immediately that this result applies also to the sum of two rotations.

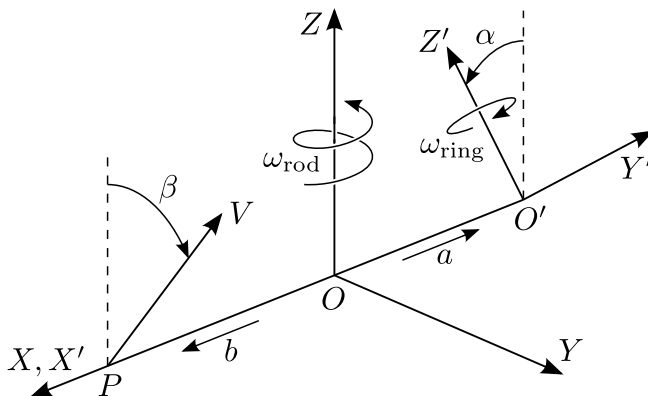


Figure 2: Kinematic relationship between a single ring and the screw rod

The kinematic design of the ring screw is therefore an exercise in finding two rotations that sum to the desired screwing motion of the rod in the nut. One of these is the rotation of a ring in its bearing, and the other is the rolling contact between this ring and the screw rod. (When one body rolls without slipping over another, its relative motion at any instant is a pure rotation about an axis passing through every point of contact.)

The analysis begins by considering the relationship between a single ring and the screw rod. To keep the analysis simple, we shall assume that the rod is moving and the nut is stationary. This implies that the rod is screwing about a stationary axis, while the ring is rotating about a different stationary axis. The rolling contact takes place about a third axis which turns out also to be stationary.

The relevant kinematics are shown in Figure 2. A Cartesian frame with axes  $X$ ,  $Y$  and  $Z$  is placed so that its  $Z$  axis lies on the screw axis of the rod, and a frame with axes  $X'$ ,  $Y'$  and  $Z'$  is placed so that  $Z'$  lies on the rotation axis of the ring. As we are interested in the common perpendicular, the two frames are positioned and oriented so that the axes  $X$  and  $X'$  both lie on the common perpendicular. These frames define two coordinate systems which we shall call *rod coordinates* (frame at  $O$ ) and *ring coordinates* (frame at  $O'$ ) respectively.

The position of  $Z'$  relative to  $Z$  is given by an offset distance  $a$  and a tilt angle  $\alpha$ , both measured in the directions shown in the diagram. Distances can be expressed in any convenient length unit, but angles are expressed in radians. The line of rolling contact is also shown, and is labelled  $V$ . This line is located at an offset  $b$  and a tilt angle  $\beta$  relative to  $Z$ , both quantities being measured in the directions shown, which are opposite to those for  $a$  and  $\alpha$ . The quantities  $a$ ,  $\alpha$ ,  $b$  and  $\beta$  are four of the five parameters that define the kinematics of the ring screw. The fifth is the pitch of the screw rod,  $h$ , which is measured in length units per radian, and is positive for a right-handed screw.

These parameters are not independent; so the next step is to find the relationships between them. In particular, we need to find the location of  $V$ , hence the values of  $b$  and  $\beta$ , in terms of the other three parameters. To this end, let us introduce two vector fields,  $\mathbf{v}_{\text{rod}}(\mathbf{r})$  and  $\mathbf{v}_{\text{ring}}(\mathbf{r})$ , where  $\mathbf{v}_{\text{rod}}(\mathbf{r})$  is the linear velocity of the point in the rod whose current position is  $\mathbf{r}$ , and  $\mathbf{v}_{\text{ring}}(\mathbf{r})$  is likewise the linear velocity of the point in the ring at position  $\mathbf{r}$ , all vectors being expressed in rod coordinates; and let  $\omega_{\text{rod}}$  and  $\omega_{\text{ring}}$  be the rotation speeds of the rod and ring, respectively. The expressions for these two vector fields are

$$\mathbf{v}_{\text{rod}}(\mathbf{r}) = \omega_{\text{rod}} \begin{bmatrix} -r_y \\ r_x \\ h \end{bmatrix} \quad (1)$$

and

$$\begin{aligned}\mathbf{v}_{\text{ring}}(\mathbf{r}) &= \omega_{\text{ring}} \begin{bmatrix} 0 \\ -\sin(\alpha) \\ \cos(\alpha) \end{bmatrix} \times \begin{bmatrix} r_x + a \\ r_y \\ r_z \end{bmatrix} \\ &= \omega_{\text{ring}} \begin{bmatrix} -\sin(\alpha)r_z - \cos(\alpha)r_y \\ \cos(\alpha)(r_x + a) \\ \sin(\alpha)(r_x + a) \end{bmatrix}.\end{aligned}\quad (2)$$

The line  $V$  is the set of points where the two velocities are the same; so we can find it simply by equating the two vector fields:

$$\begin{bmatrix} -r_y \\ r_x \\ h \end{bmatrix} = \frac{\omega_{\text{ring}}}{\omega_{\text{rod}}} \begin{bmatrix} -\sin(\alpha)r_z - \cos(\alpha)r_y \\ \cos(\alpha)(r_x + a) \\ \sin(\alpha)(r_x + a) \end{bmatrix}.\quad (3)$$

There are three things to note about this equation. First, the two speeds appear only as a speed ratio, which means that the actual speed is irrelevant and only the ratio matters. So let us define the speed ratio as follows:

$$\varpi = \frac{\omega_{\text{ring}}}{\omega_{\text{rod}}}.\quad (4)$$

Second, (3) is a set of three equations in four unknowns ( $r_x$ ,  $r_y$ ,  $r_z$  and  $\varpi$ ), so there is a single infinity of solutions. Third, as we already know that the solutions are the set of points on  $V$ , and that  $V$  is perpendicular to the  $X$  axis, it follows that

$$b = r_x \quad \text{and} \quad \tan(\beta) = \frac{r_y}{r_z}.\quad (5)$$

We can solve (3) for  $b$  and  $\tan(\beta)$  as follows. First, subtract  $\sin(\alpha)$  times the second row from  $\cos(\alpha)$  times the third row, giving

$$\cos(\alpha)h - \sin(\alpha)r_x = 0,$$

hence

$$r_x = h/\tan(\alpha) = b\quad (6)$$

using (5). Next, add  $\cos(\alpha)$  times the second row to  $\sin(\alpha)$  times the third row, giving

$$\cos(\alpha)r_x + \sin(\alpha)h = \varpi(r_x + a),\quad (7)$$

which leads to the following formula for  $\varpi$ :

$$\begin{aligned}\varpi &= \frac{\cos(\alpha)r_x + \sin(\alpha)h}{r_x + a} \\ &= \frac{(\cos(\alpha)/\tan(\alpha) + \sin(\alpha))h}{h/\tan(\alpha) + a} \\ &= h/(h\cos(\alpha) + a\sin(\alpha))\end{aligned}\quad (8)$$

using (6). Finally, by rearranging the first row of (3) as

$$(1 - \varpi\cos(\alpha))r_y = \varpi\sin(\alpha)r_z$$

we can calculate  $\tan(\beta)$  as follows:

$$\begin{aligned}\tan(\beta) &= \frac{\varpi \sin(\alpha)}{1 - \varpi \cos(\alpha)} \\ &= \frac{h \sin(\alpha)/(h \cos(\alpha) + a \sin(\alpha))}{1 - h \cos(\alpha)/(h \cos(\alpha) + a \sin(\alpha))} \\ &= \frac{h \sin(\alpha)}{a \sin(\alpha)} = \frac{h}{a}\end{aligned}\tag{9}$$

(using (5) and (8)). We now have the two kinematic design equations of the ring screw mechanism, which can be written in a symmetrical form as

$$\tan(\alpha) = \frac{h}{b} \quad \text{and} \quad \tan(\beta) = \frac{h}{a}.\tag{10}$$

Observe that for any given screw pitch the location of  $Z'$  uniquely determines the location of  $V$  and vice versa. If the screw rod is right-handed (as shown in Figure 2) then all five parameters are positive; otherwise  $a$  and  $b$  are positive but  $h$ ,  $\alpha$  and  $\beta$  are negative. We shall assume a right-handed screw from here on, on the grounds that a left-handed ring screw mechanism is simply the mirror image of a right-handed one.

A few other useful equations can be deduced from the above analysis, such as

$$\sin(\alpha) = h/\sqrt{h^2 + b^2}, \quad \cos(\alpha) = b/\sqrt{h^2 + b^2},\tag{11}$$

and

$$\varpi = \frac{\sqrt{h^2 + b^2}}{a + b}.\tag{12}$$

### 3 Contact Surfaces

Having solved the kinematics of the ring screw mechanism, the next step is to define the shapes of the contact surfaces on the rod and the ring. If they always make line contact along the line  $V$  regardless of the orientation of the ring or the location of the rod along its helix, then it follows that the contact surface on the ring must be the surface of revolution formed by sweeping  $V$  around  $Z'$ , and that the one on the rod must be the surface formed by sweeping  $V$  around  $Z$  in a helical path of pitch  $h$ .

In the case of the ring, the result is a ruled surface called a hyperboloid of one sheet, and an example of such a surface is shown in Figure 3. As can be seen from Figure 2,  $V$  is at a radius

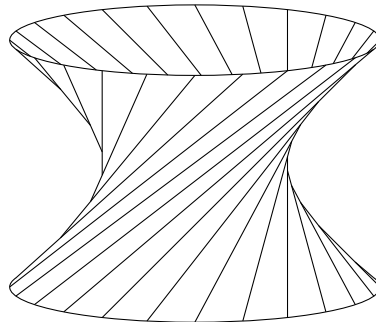


Figure 3: Example of a hyperboloid of one sheet

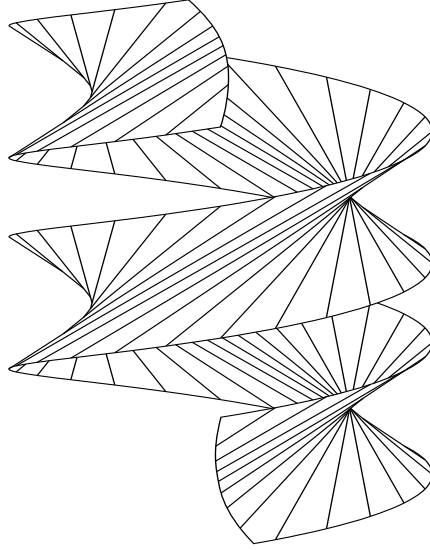


Figure 4: Example of an oblique open ruled generalized helicoid

of  $a + b$  from  $Z'$  and a tilt angle of  $\alpha + \beta$ ; so the equation of the ring's surface, expressed in ring coordinates, is

$$x'^2 + y'^2 = (a + b)^2 + \tan(\alpha + \beta)^2 z'^2. \quad (13)$$

In the case of the rod, the result is a ruled surface called an oblique open ruled generalized helicoid, which we shall abbreviate to 'helicoid'. An example of this surface is shown in Figure 4. A surface of this kind is best described using a pair of surface coordinates,  $\theta$  and  $s$ , as defined in Figure 5(a). In terms of these variables, the equation of the surface (in rod coordinates) is

$$\begin{aligned} x &= b \cos(\theta) - s \sin(\beta) \sin(\theta) \\ y &= b \sin(\theta) + s \sin(\beta) \cos(\theta) \\ z &= h \theta + s \cos(\beta). \end{aligned} \quad (14)$$

However, for the purpose of cutting a screw thread, we need also the equation of the thread profile, which is the curve of intersection between the helicoid and the  $X$ - $Z$  plane (or any other plane containing the  $Z$  axis). We can obtain this curve by setting  $y = 0$  and solving the triangle in Figure 5(b), which gives

$$\sin(\theta) = \frac{-s \sin(\beta)}{x} \quad \text{and} \quad \cos(\theta) = \frac{b}{x}, \quad (15)$$

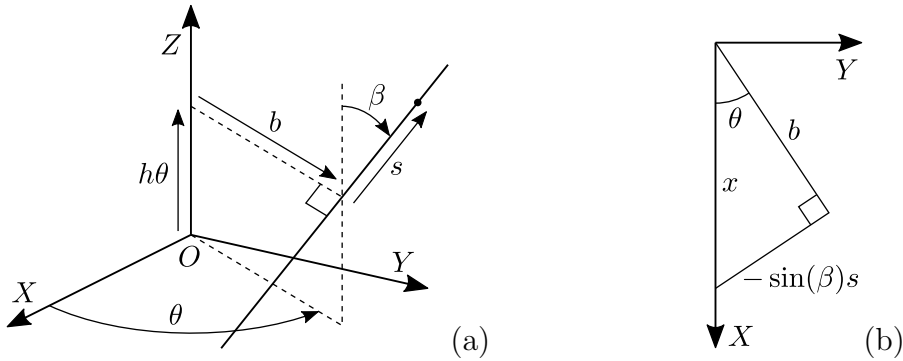


Figure 5: Definition of the coordinates  $\theta$  and  $s$  used to describe the contact surface on the screw rod (a), and the triangle used to find the thread profile curve (b)

hence

$$s = \frac{-x \sin(\theta)}{\sin(\beta)} = \frac{-b \tan(\theta)}{\sin(\beta)} = \frac{-a b \tan(\theta)}{h \cos(\beta)}. \quad (16)$$

(The last step uses (10).) Substituting these expressions into (14) gives the thread profile as

$$\begin{aligned} x &= b / \cos(\theta) \\ z &= h \theta - \frac{ab}{h} \tan(\theta) \end{aligned} \quad (17)$$

expressed as a function of  $\theta$  only.

A few remarks are in order at this point. First, it can be seen from (13) that the ring's contact surface collapses into a plane if  $\alpha + \beta = \pi/2$ . Second, the curve in (17) has a cusp at  $\theta = 0$  if  $ab = h^2$ , and it self-intersects if  $ab < h^2$ . So a necessary condition for the screw rod's surface to be practical is

$$ab > h^2. \quad (18)$$

It turns out that this is also a sufficient condition to prevent the ring's surface from collapsing because it implies  $\alpha + \beta < \pi/2$ . It also implies  $\varpi < 1$ , meaning that the rings turn more slowly than the rod. The latter can be proved as follows:

$$1 > \frac{b}{a+b} = \frac{ab+b^2}{(a+b)^2} > \frac{h^2+b^2}{(a+b)^2} = \varpi^2. \quad (19)$$

Equations (13) and (14) also show us that the shape of the rod's contact surface is a function of the three parameters  $b$ ,  $\beta$  and  $h$ , whereas the shape of the ring's contact surface depends on only two parameters,  $a+b$  and  $\alpha+\beta$ . Therefore,

1. for any one given rod shape there is exactly one corresponding ring shape; and
2. for any one given ring shape there is a one-parameter family of rod shapes that will work with this ring.

It follows that every ring in a ring screw mechanism must have the same shape, offset and tilt angle. They can differ only in their placement around the rod's helix. The rings in Figure 1, for example, are placed 2.5 turns apart.

To find the set of rods that will work with a given ring surface, the first step is to define the following quantities:

$$c = \frac{a+b}{2}, \quad d = \frac{a-b}{2} \quad \text{and} \quad \gamma = \alpha + \beta. \quad (20)$$

$c$  and  $\gamma$  are known from the parameters of the ring surface, and the objective is to find an expression for  $d$  in terms of  $c$ ,  $\gamma$  and  $h$ . (So  $h$  is the parameter that can be varied.) Using (10) and a standard trigonometric formula, we get

$$\begin{aligned} \tan(\gamma) &= \frac{\tan(\alpha) + \tan(\beta)}{1 - \tan(\alpha) \tan(\beta)} \\ &= \frac{h/b + h/a}{1 - h^2/ab} = \frac{ah + bh}{ab - h^2} \\ &= \frac{2ch}{c^2 - d^2 - h^2}, \end{aligned} \quad (21)$$

hence

$$d = \pm \sqrt{c^2 - 2ch / \tan(\gamma) - h^2}. \quad (22)$$

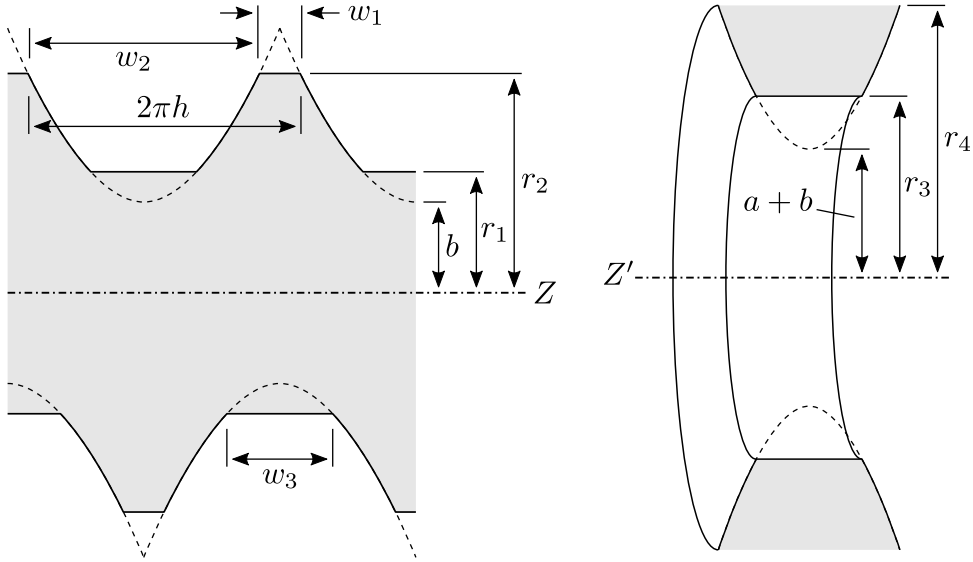


Figure 6: Screw rod and ring dimensions

The sign ambiguity in  $d$  reflects the symmetry between  $a$  and  $b$  in (10). As  $d$  must be a real number, there is an upper limit to the value of  $h$  given by

$$h_{\max} = \frac{c - c \cos(\gamma)}{\sin(\gamma)}. \quad (23)$$

Equation (22) works for any  $h$  in the range  $0 < h \leq h_{\max}$ ; but there will be a practical lower limit to  $h$  which is determined by other design considerations.

## 4 Defining the Shapes

Figure 6 shows the relevant shape details of the rod and ring. In a practical design procedure, the designer would specify the outer radius of the rod,  $r_2$ , the distance between adjacent thread grooves,  $w_1$ , the pitch of the screw in units of lead per revolution ( $2\pi h$ ) and the kinematic parameter  $b$ . These four quantities are enough to define the shapes of the rod and ring; so a computer program could be written that accepts these quantities as inputs and works out all of the other details. Such a program would proceed as follows.

1. The width of the thread groove at the outer radius is  $w_2 = 2\pi h - w_1$ .
2. Equation (17) gives us another expression for  $w_2$  from which  $a$  can be calculated:

$$w_2 = 2\left(\frac{ab}{h} \tan(\theta_{r_2}) - h\theta_{r_2}\right)$$

where  $\theta_{r_2} = \cos^{-1}(b/r_2)$  is the value of  $\theta$  at the outer radius. Bringing  $a$  over to the left gives

$$a = \frac{h(h\theta_{r_2} + w_2/2)}{b \tan(\theta_{r_2})}. \quad (24)$$

3. Once  $a$  has been calculated, check that the values of  $a$ ,  $b$  and  $h$  satisfy (18). If they do not then the design is not feasible and the program must report an error and stop.
4. Calculate  $\alpha$  and  $\beta$  from  $a$ ,  $b$ ,  $h$  and (10). These angles are both in the range  $0$  to  $\pi/2$ , and are therefore determined uniquely by their tangents.



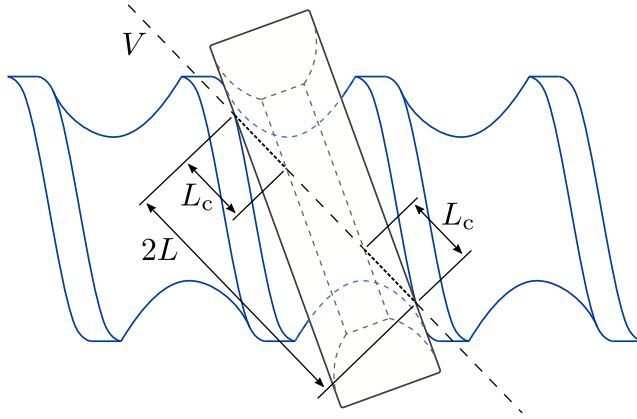


Figure 7: A view down the  $X$  axis showing where physical contact takes place between the rod and the ring. Observe that the ring is narrower than the groove in the rod, and that it is tilted more than the helix angle of the rod at its outer radius. Observe also that  $V$  is tilted even more than the ring. These are characteristic features of the ring screw mechanism.

- Given that the rod's contact surface ends at the rod's outer radius  $r_2$ , it follows that the physical contact between the rod and the ring is confined to a finite segment of  $V$ , which is shown and labelled  $2L$  in Figure 7.  $L$  is the value of  $s$  in (14) that corresponds to a rod radius of  $r_2$ , so it can be obtained from the triangle in Figure 5(b) by setting  $x = r_2$ :

$$L = \sqrt{r_2^2 - b^2} / \sin(\beta). \quad (25)$$

- Given that the rod ends at  $r_2$ , it follows that the ring loses contact with the rod at a radius  $r_4$  which is the distance between  $Z'$  and the point on  $V$  at a distance  $L$  from  $P$ . The formula for  $r_4$  is

$$r_4 = \sqrt{(a + b)^2 + (L \sin(\alpha + \beta))^2}. \quad (26)$$

The shape of the ring beyond  $r_4$  depends on how it fits into its bearing.

- Next, the program must check whether the ring clears the outer radius of the rod on the side opposite to  $V$ . If there is no interference between the rod and the ring then set  $r_3 = a + b$  and  $r_1 = b$ . Otherwise, the ring's contact surface must be cut back to a radius  $r_3 > a + b$  which is the smallest radius at which the ring clears the rod with a small safety margin to account for manufacturing tolerances. A formula for this step is not currently known, so the program must use a numerical procedure instead.
- If the ring is cut back in the previous step then it no longer reaches the bottom of the thread groove. This allows the groove to be filled in to a radius  $r_1 > b$ , as shown in Figure 6, given by the formula

$$r_1 = \sqrt{b^2 + (L - L_c)^2 \sin(\beta)^2} - \epsilon \quad (27)$$

where  $\epsilon$  is a small clearance to allow for manufacturing tolerances. In this equation,  $L_c$  is the length of the line of physical contact between the cut-back ring and the rod, as shown in Figure 7, and is given by the formula

$$L_c = L - \sqrt{r_3^2 - (a + b)^2} / \sin(\alpha + \beta). \quad (28)$$

This fill-in is optional. Its effect is to increase the stiffness of the rod, and therefore also its resonant frequency, but it does also increase the mass. It does not affect the function of the ring screw in any other way.

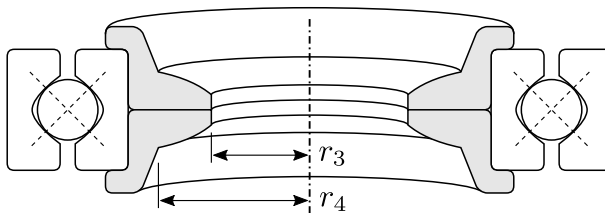


Figure 8: Ring construction and mounting details

9. Finally, manufacturers of custom screw rods may ask their customers to provide the value of the ‘root flat’, which is the width of the flat part at the bottom of the thread curve, and is labelled  $w_3$  in Figure 6. The formula for this quantity is

$$w_3 = 2\left(\frac{ab}{h} \tan(\theta_{r1}) - h\theta_{r1}\right) \quad (29)$$

where  $\theta_{r1} = \cos^{-1}(b/r_1)$  is the value of  $\theta$  in (17) at the fill-in radius.

## 5 Construction and Placement of Rings

Figure 8 shows the ring construction and mounting method that has been used on every prototype so far. As can be seen, the ring is manufactured in two halves which are pressed into a four-point-contact bearing. A transitional or slight interference fit is used, or alternatively a close locational fit and an optional spot of glue. A four-point-contact bearing is used because the rings will experience significant bending moments, and the bearing must be able to resist them. We used bearings from the Q 1800 series, available from SBN Wälzlager [21], which can support forces above 1kN and operate at speeds above 20,000rpm.

Every ring has the same shape, tilt and offset, but a different position along the helix of the rod. So the placement of rings in a nut can be specified either by the helical angle or by the number of turns between them. For example, the rings in the nut in Figure 1 are  $5\pi$  radians or 2.5 turns apart.

Three rings is the minimum number needed to constrain the rod to a helical motion relative to the nut, although fewer rings could be used if external kinematic constraints are present. For example, if the rod is constrained to rotate about a fixed axis, and the nut is constrained to translate parallel to that axis, then only a single ring is required. In general, it is best to use the smallest number of rings that will provide the necessary kinematic constraints and deliver the required thrust force. Any ring beyond the minimum adds bulk and weight to the nut, and also reduces the efficiency because ball bearings exhibit a small amount of viscous friction.

The only sensible arrangement for a three-ring nut is the one shown in Figure 1. In this arrangement the rings are  $n + 0.5$  turns apart, where  $n$  is the smallest integer that will work. This nut is smaller, lighter and more efficient than a nut with more rings, but it suffers from a load imbalance: the load on the middle ring is twice that on the other two. This imbalance can be avoided by using a four-ring nut like that shown in Figure 9. The rings in this nut are placed 2.5, 2 and 2.5 turns apart, but more generally they would be placed  $n + 0.5$ ,  $m$  and  $n + 0.5$  turns apart, where  $m$  and  $n$  are the smallest integers that will work.

The arrangement shown in Figure 9 is the only sensible one for a four-ring nut; but with five or more rings there are a variety of possibilities. Figure 10 shows one possible design for a five-ring nut. This figure presents a view down the rod’s  $Z$  axis showing the directions of the  $X$  axes of the five rings numbered 1 to 5 from farthest to nearest. The angles between the rings consist of two complete revolutions around the helix plus  $\phi_2$ ,  $\phi_1$ ,  $\phi_1$  and  $\phi_2$ , respectively, where

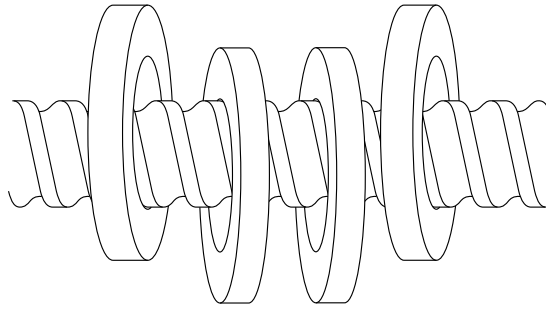


Figure 9: Example arrangement of four rings in a nut

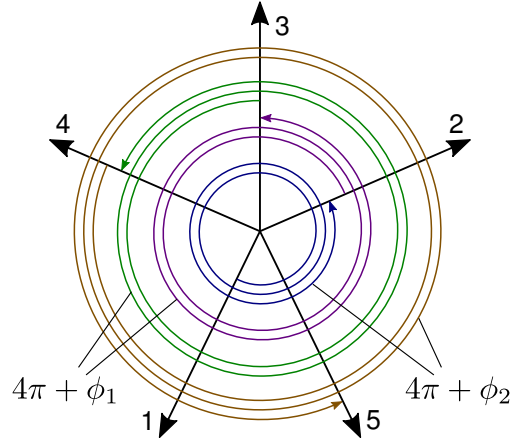


Figure 10: Example arrangement of five rings in a nut presented as a view down the rod's  $Z$  axis showing the directions of the five rings'  $X$  axes and the angles between them

$\phi_1 = 66.5^\circ$  and  $\phi_2 = 139.5^\circ$ . The general method to find designs like this is to assume that each ring is exerting a unit force on the rod along its  $X$  axis and look for ring placements that result in static equilibrium. This method finds designs in which the rings are equally loaded.

## 6 Internal Forces

This section examines the contact forces between the rod and the rings, and their relationship to the thrust force produced by the ring screw mechanism. It will be assumed that the ring has been cut away as shown in Figure 7 (which is usually the case in a practical design) so that each ring makes contact with the rod along two line segments of length  $L_c$ . We shall call these segments  $A$  and  $B$ , corresponding to positive and negative values of  $s$ , respectively, as defined in Figure 5(a). It will also be assumed that the forces transmitted through any one contact segment can be approximated as a single force passing through a point somewhere in the interior of the segment.

Let  $\mathbf{p}(s)$  be a point on  $V$  at a distance  $s$  from  $P$ , and let  $\mathbf{n}(s)$  be a unit vector along the local contact normal at  $\mathbf{p}(s)$  in the direction pointing out of the ring and into the rod. This vector can be calculated as follows:

$$\mathbf{n}(s) = \frac{\mathbf{v} \times \mathbf{h}(s)}{|\mathbf{v} \times \mathbf{h}(s)|} \quad (30)$$

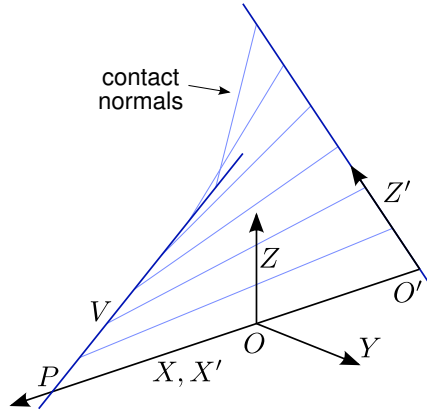


Figure 11: Contact normals pass through both  $V$  and  $Z'$ , and are at right angles to  $V$

where  $\mathbf{v} = [0, \sin(\beta), \cos(\beta)]^T$  is a unit vector in the direction of  $V$ , and

$$\mathbf{h}(s) = \mathbf{v}_{\text{rod}}(\mathbf{p}(s))/\omega_{\text{rod}} = \begin{bmatrix} -s \sin(\beta) \\ b \\ h \end{bmatrix} \quad (31)$$

is a vector that is tangent at  $\mathbf{p}(s)$  to a helix around  $Z$  of pitch  $h$  that passes through  $\mathbf{p}(s)$ . So  $\mathbf{h}(s)$  has the same direction as  $\mathbf{v}_{\text{rod}}(\mathbf{p}(s))$  when  $\omega_{\text{rod}}$  is positive. Both  $\mathbf{v}$  and  $\mathbf{h}(s)$  are tangent to the rod's surface at  $\mathbf{p}(s)$ , so  $\mathbf{n}(s)$  must be perpendicular to both of them, hence the cross product in (30).

The line of the contact normal at  $\mathbf{p}(s)$  can be described geometrically as the line that passes through  $\mathbf{p}(s)$  at right angles to  $V$ , and also passes through  $Z'$ . The latter follows from the fact that  $\mathbf{n}(s)$  is perpendicular to both the rod's and the ring's contact surface at  $\mathbf{p}(s)$ , and the latter is a surface of revolution about  $Z'$ . Figure 11 shows some of these contact normals.

From a screw-theoretic point of view, we can say that the set of contact normals between any one ring and the rod spans a three-dimensional subspace of wrench space that is reciprocal to the following three twists: a pure rotation about  $V$ , a pure translation along  $V$  and a pure rotation about  $Z'$ . It is also reciprocal to a twist of pitch  $h$  about  $Z$  (i.e., the screwing motion of the rod) because that twist is a linear combination of the two rotations.

In general, the contact force at  $\mathbf{p}(s)$  will have both a normal and a tangential component. The former contributes to the thrust force, while the latter maintains the rolling contact between the rod and the ring. In particular, the tangential component accelerates the ring in response to the rod's acceleration, and it overcomes the small amount of friction in the ring's bearing.

It is important that the ring does not slip; so there must always be enough normal force on at least one of the two contact segments to ensure that the necessary tangential forces are strictly inside the friction cone. This is accomplished by preloading the nut. In the tested prototype, preload was accomplished by leaf springs that pressed the rings into the thread groove while holding their tilt angles at the correct value [13]. This is the simplest arrangement to manufacture, but a preload of this kind exerts a larger bending moment on the rod than would be the case if the preload were designed to both press and twist the ring into the rod, the twist direction being counter-clockwise as viewed in Figure 7.

The normal component of contact force at  $\mathbf{p}(s)$  is a scalar multiple of  $\mathbf{n}(s)$ , and it is the  $z$  component of this force that contributes to the ring screw's thrust force. We are therefore interested in the  $z$  component of  $\mathbf{n}(s)$ . The formula for this quantity is

$$n_z(s) = \frac{s \sin(\beta)}{\sqrt{(h - ab/h)^2 + s^2}}. \quad (32)$$

This quantity is zero at  $s = 0$ , and it approaches asymptotically to  $\pm \sin(\beta)$  at increasing positive and negative values, respectively, of  $s$ . In the prototypes that have been designed so far,  $n_z(s)$  takes values of around 0.6 to 0.7 at values of  $s$  in contact segment  $A$ , and values of around  $-0.6$  to  $-0.7$  in contact segment  $B$ . This means that every 1N of contact normal force beyond the preload force on contact segment  $A$  contributes around 0.6N to 0.7N to the thrust force, and every extra 1N on segment  $B$  contributes around  $-0.6$ N to  $-0.7$ N. Figures like these show that total thrust forces (from multiple rings) substantially in excess of 1kN are feasible using relatively small, light-weight, off-the-shelf bearings.

## 7 Conclusion

This document has described a new mechanical transmission mechanism that performs the same function as a ball screw but can operate at higher speeds. The new mechanism employs a nut containing rings that are mounted in ball bearings and make rolling contact with a screw rod inserted into the nut. The special feature of this mechanism, in addition to its high operating speed, is that the rings make theoretically pure rolling line contact with the rod, thereby permitting the mechanism to produce large thrust forces and operate at high efficiency. An experimental prototype was tested in [13], and another is currently being installed in an experimental robot called Skippy [10]. Further details on the ring screw mechanism can be found at [9].

## Acknowledgements

The CAD render in Figure 1 was produced by E. Heijmink.

## References

- [1] Junhyeok Ahn, Donghyun Kim, Seunghyeon Bang, et al., “Control of A High Performance Bipedal Robot using Viscoelastic Liquid Cooled Actuators,” *2019 IEEE-RAS 19th Int. Conf. Humanoid Robots (Humanoids)*, Toronto, Canada, Oct. 15–17, 2019, pp. 146–153. DOI: 10.1109/Humanoids43949.2019.9035023
- [2] R. S. Ball, *A Treatise on the Theory of Screws*. London: Cambridge University Press, 1900. Republished 1998.
- [3] Rudolf Betzing et al., *Screw Drive With Turning Rings*. European Patent no. EP0122596 A1, issued 24 Oct. 1984.
- [4] O. Bottema & B. Roth, *Theoretical Kinematics*. New York: Dover Publications, Inc., 1990.
- [5] A. Edsinger-Gonzales and J. Weber, “Domo: A Force Sensing Humanoid Robot for Manipulation Research,” *4th IEEE/RAS Int. Conf. Humanoid Robots*, Santa Monica, CA, 10–12 Nov. 2004, vol. 1, pp.273–291. DOI: 10.1109/ICHR.2004.1442127
- [6] Roy Featherstone, *Linear Drive Mechanism of the Screw and Nut Type With Perfect Rolling Contact*. Japanese Patent no. JP6400860, issued 3 Oct. 2018.
- [7] Roy Featherstone, *Linear Drive Mechanism of the Screw and Nut Type With Perfect Rolling Contact*. European Patent no. EP3295058(A1), issued 22 May 2019.

- [8] Roy Featherstone, *Linear Drive Mechanism of the Screw and Nut Type With Perfect Rolling Contact*. United States Patent no. US10364871(B2), issued 30 July 2019.
- [9] Roy Featherstone, *The Ring Screw Mechanism*. <http://royfeatherstone.org/ringscrew>. Accessed Feb. 2023.
- [10] Roy Featherstone, *The Skippy Project*. <http://royfeatherstone.org/skippy>. Accessed Feb. 2023.
- [11] Florent Forget, Kevin Giraud-Esclasse, Rodolphe Gelin, et al., “Implementation, Identification and Control of an Efficient Electric Actuator for Humanoid Robots,” *Proc. 15th Int. Conf. Informatics in Control, Automation and Robotics (ICINCO 2018)*, Porto, Portugal, 29–31 July 2018, vol. 2, pp. 29–38.
- [12] Robert Gärtner, *Screw Jack*. United States Patent no. 4,856,356, issued 15 Aug. 1989.
- [13] Elco Heijmink, *The Ring Screw: Modelling, Development and Evaluation of a Novel Screw Transmission*. MSc Thesis, Delft University of Technology, August 2018. <http://resolver.tudelft.nl/uuid:e7e28551-0410-4303-a10a-92ec88aa91a4>
- [14] Konrad Hoh, *Linear Drive With a Screw and a Rolling-Ring Nut*. German Patent no. DE3225496 A1, issued 12 Jan. 1984.
- [15] K. H. Hunt, *Kinematic Geometry of Mechanisms*. Oxford: Oxford Univ. Press, 1978.
- [16] Maxon Motor Ag., Maxon Online Shop. Accessible via [www.maxongroup.com](http://www.maxongroup.com). Accessed Feb. 2023.
- [17] Viktor L. Orekhov, Coleman S. Knabe, Michael A. Hopkins and Dennis W. Hong, “An Unlumped Model for Linear Series Elastic Actuators with Ball Screw Drives,” *2015 IEEE/RSJ Int. Conf. Intelligent Robots and Systems (IROS)* Hamburg, Germany, Sept. 28 – Oct. 2 2015, pp. 2224–2230. DOI: 10.1109/IROS.2015.7353675.
- [18] Nicholas Paine and Luis Sentis, “A New Prismatic Series Elastic Actuator with Compact Size and High Performance,” *IEEE Int. Conf. Robotics and Biomimetics (ROBIO 2012)*, Guangzhou, China, 11–14 Dec. 2012, pp. 1759–1766. DOI: 10.1109/ROBIO.2012.6491222
- [19] Nicholas Paine, Sehoon Oh and Luis Sentis, “Design and Control Considerations for High-Performance Series Elastic Actuators,” *IEEE/ASME Trans. Mechatronics*, 19(3):1080–1091, June 2014. DOI: 10.1109/TMECH.2013.2270435
- [20] Osamu Sano, *Movement Transforming Device and Power Steering Apparatus*. United States Patent no. 6,244,125, issued 12 June 2001.
- [21] SBN Wälzlager GmbH & Co. KG, Home page (in German). <https://www.sbn.de>. Accessed Feb. 2023.
- [22] August Steinmeyer GmbH & Co. KG, Steinmeyer Ball Screws Online Catalog. [https://drive.steinmeyer.com/kataloge/steinmeyer\\_main\\_catalogue/](https://drive.steinmeyer.com/kataloge/steinmeyer_main_catalogue/). Accessed Feb. 2023.
- [23] Wikipedia, *Roller Screw*. [https://en.wikipedia.org/wiki/Roller\\_screw](https://en.wikipedia.org/wiki/Roller_screw). Accessed Feb. 2023.